Activity report on the project "*Microplastic concentration in sediments and waters of Matagorda and San Antonio Bays: Initial assessment and mitigation plans*"

PIs: Cornel Olariu and Zhanfei Liu, The University of Texas at Austin

PhD students: Will Bailey, Xiangtao Jiang

Postdoctoral scholar: Kaijun Lu

Undergraduate students: Ella Clark, Lilian Alameda and Enrico de Cesare Leite

Period: July 1st, 2023, to December 30th, 2023 – Continuation of laboratory microplastics separation, opening of new cores, work on sediment grain size analysis, and initiation of total organic content (TOC) determination. Will Bailey presented some of the project results at the American Geophysical Union Conference in San Francisco.

During the two quarter from July to December 2023, we continued working on the separation of microplastics from sediments and opened all cores collected in previous field campaigns. Cores were photographed (Figures 1 to 5), described, and sampled for sediment grain size, TOC, and microplastics. We continued analyzing grain size and TOC in the sampled sediments collected in previous field campaigns, focusing on the remaining cores. Sediments from the top, bottom, and middle of each core were sampled for initial microplastics analysis. Additionally, we commenced digitizing old marine navigational charts (bathymetry maps) of Matagorda Bay to understand sediment accumulation patterns. In December 2023, we conducted fieldwork and collected data in the Colorado Delta area. Below, we discuss new observations on sediment core structures, grain size, and TOC that are important for understanding of the microplastic dynamics in Matagorda Bay.

Observations on sediment cores:

The newly opened cores vary in depth from 20 cm to over 1 m (Figures 1 to 5) and are predominantly muddy, with clay and silt as dominant grain sizes. However, some cores have sandy laminae and lenses, some are rich in organic material (for example, cores 4 and 5 in Fig. 1), or have layers of shell fragment (for example, cores 34 WP66 and 34 WP82 in Fig. 4), and most cores have mm-sized shells dispersed throughout muddy deposits. It is common to have sand beds mixed with fragmented oysters (e.g. core 14 in Fig. 3). In some instances, larger oyster shell fragments are present (core 25 in Fig. 3 or core 35 in Fig. 5). In a few cores, bioturbation can be recognized by the presence of rounded and subrounded geometries filled with coarser sediments (core 15 in Fig. 3). What the cores seem to lack, or are obviously missing in core photos or through visual observations, are fine-laminated sediments with typical clay-silt or silt-sand alternations (see Figs. 1 to 5). The thin-laminated deposits are typically formed in low-energy bays and lakes, and the variability in laminae (mud-sand or organic-rich vs organic-poor or shell-rich vs shell-poor) represents seasonal changes in energy levels or environmental conditions. The lack of laminae and

record of seasonal changes are likely consequences of the relatively shallow depth of the bay (less than 4 m), in which bottom sediments are either (1) mixed by fauna through bioturbation, or (2) continuously reworked by wind-generated waves and bay currents, with sediments resuspended in the water column and transported throughout the bay, or (3) repeatedly stirred by anthropic activities such as fishing and shrimping, disturbing bottom sediments.

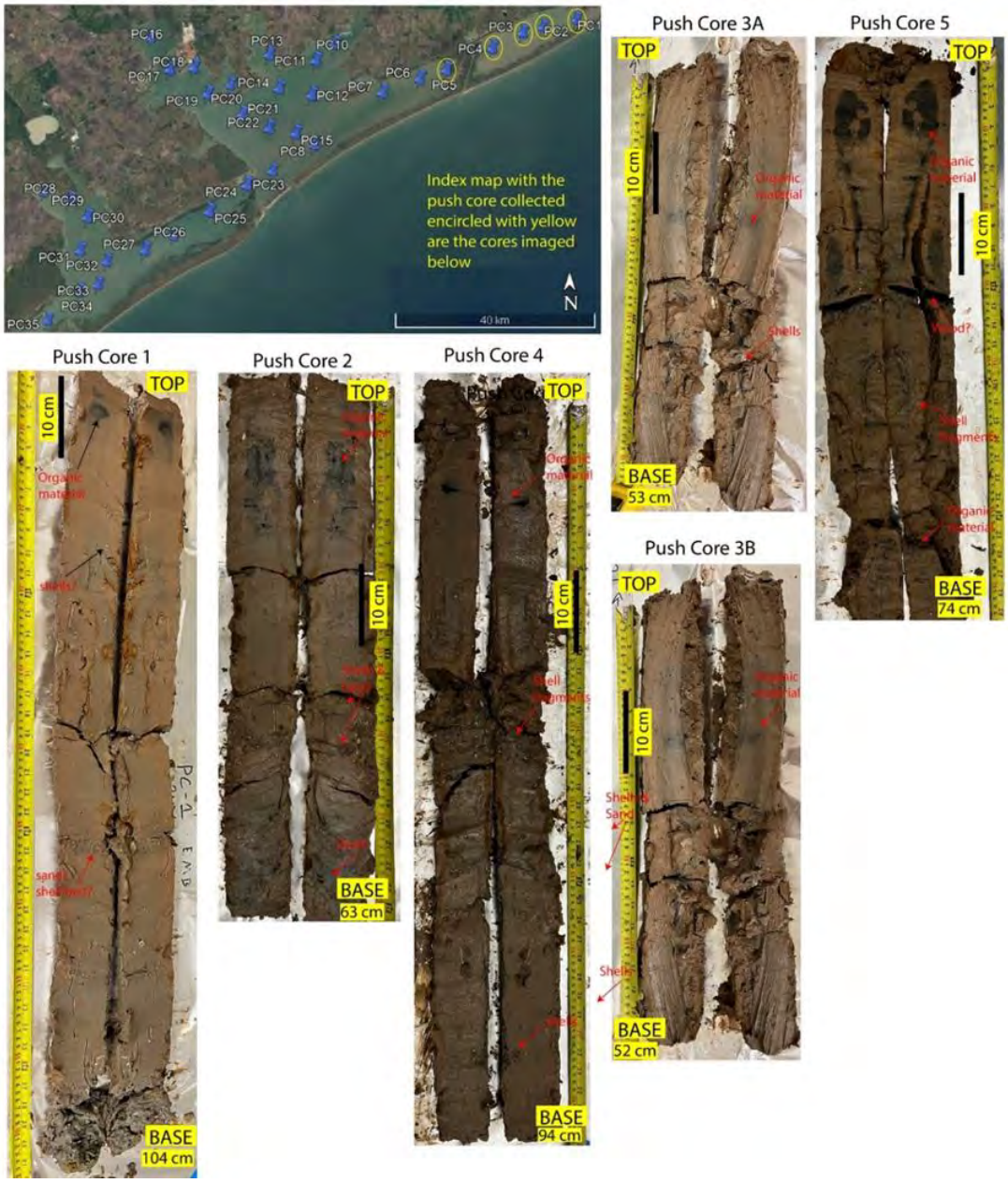

Figure 1: Photos of sediment cores 1, 2, 3A, 3B, 4, and 5 from East Matagorda. The top-left map indicates the location of the cores. Cores are dominated by muddy sediments with some thin laminae of sand or shells. Note that cores 4 and 5 have more organic content (fragments or dark grey mud) and are also located closer to the Colorado river outlet, which might deliver the organic material.

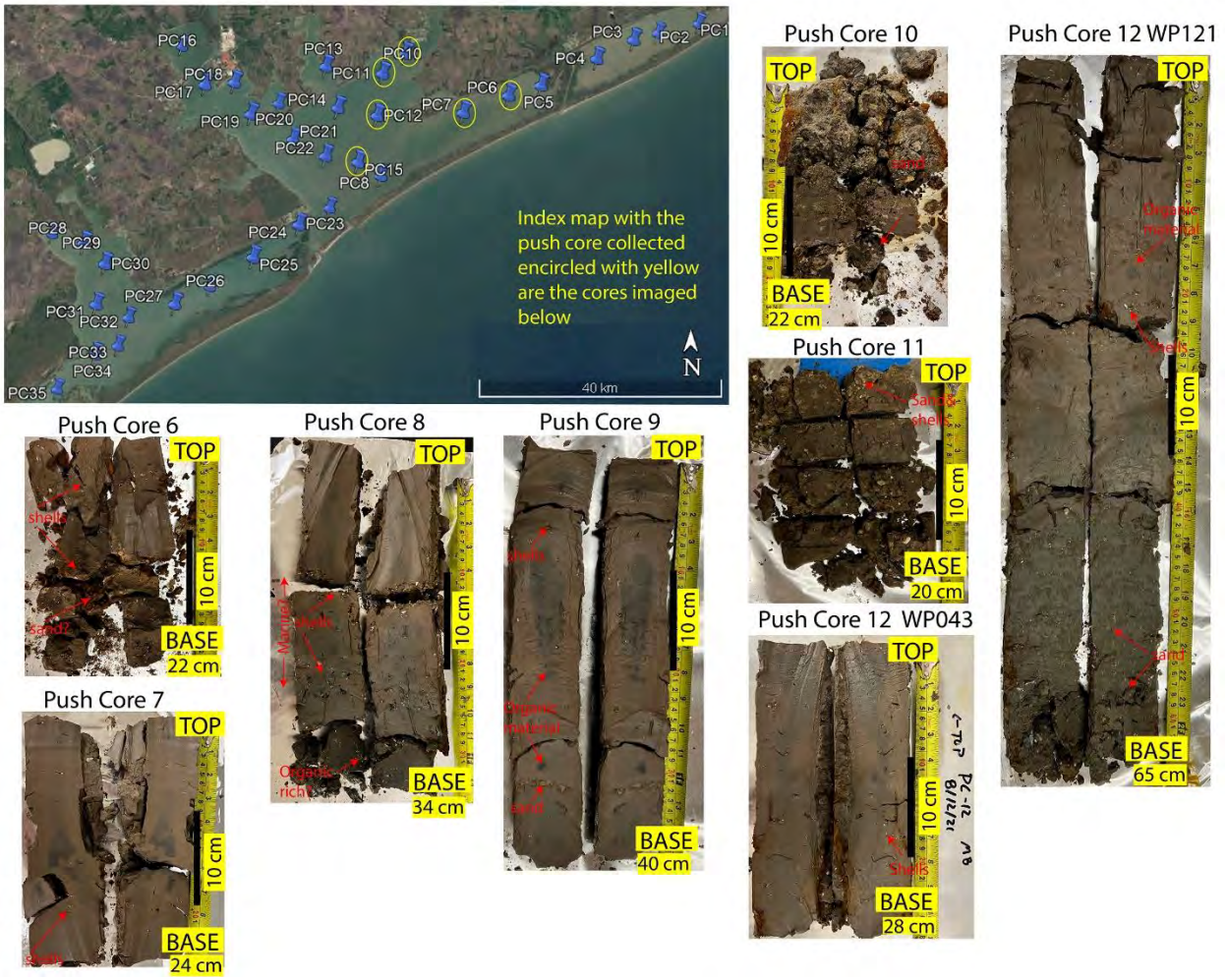

Figure 2: Photos of sediment cores 6, 7, 8, 9, 10, 11, 12 (at two locations) from Matagorda Bay. The top-left map indicates the location of the cores. Cores are dominated by muddy sediments, with two exceptions, cores 10 and 11, which are muddy sands. These two cores are located in the northeastern part of Matagorda Bay at the mouth of Tres Palacios Bay, where the shoreline is erosive. This area is also dominated by intensive shipping activity, where reoccurring dredging activity and ship-induced sediment resuspension may might affect the sediments deposited in the bay.

Figure 3. Photos of the sediment cores 13, 14, 15, 18, 20, 21, 22, 25, 26 from Matagorda Bay. Top left map indicate the location of the cores. Cores are dominated by muddy sediments with two exceptions, cores 24 and 25, which are muddy sands. These cores are located proximal to Pass Cavallo, where a flood tide delta composed of marine sands dominates the area. Well preserved and obvious bioturbtion filled with sand is visible in core 15.

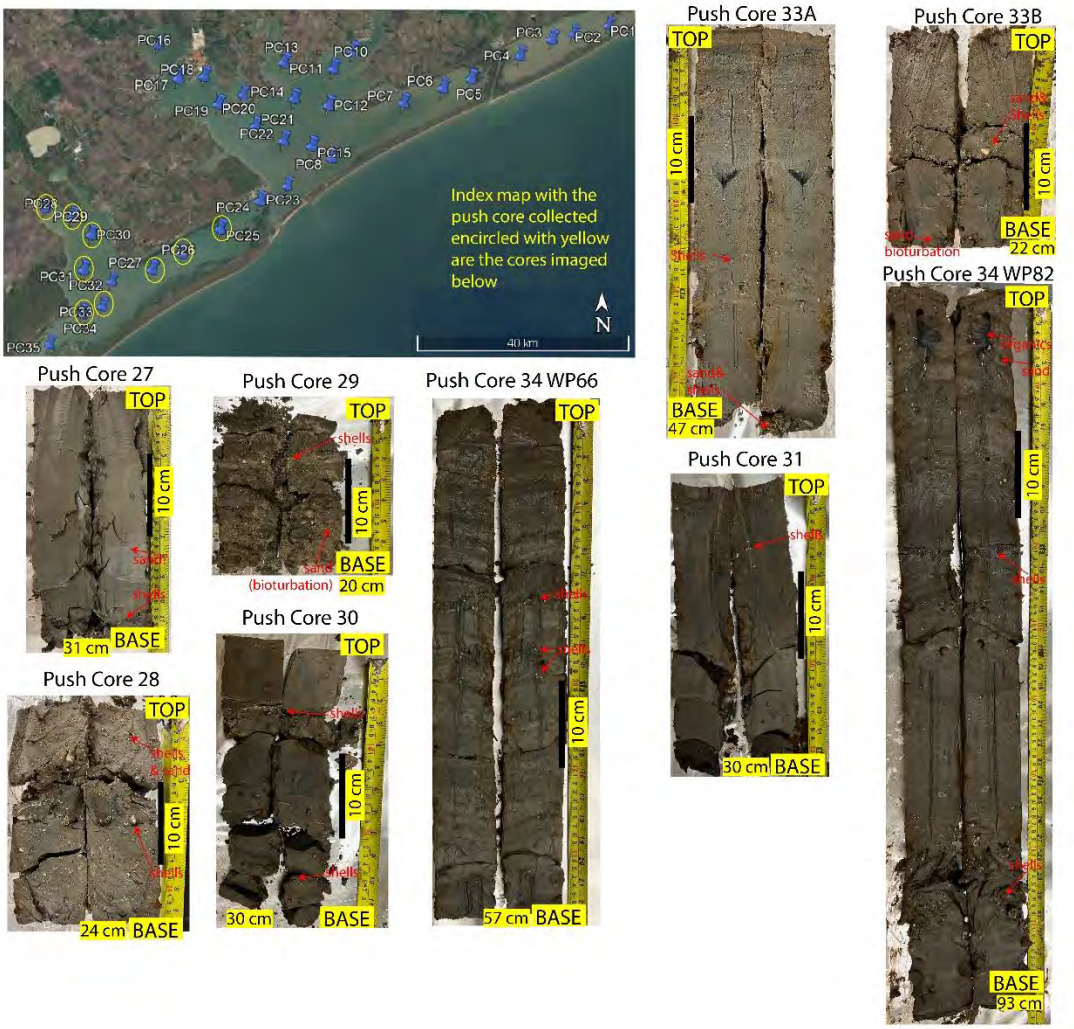

Figure 4. Photos of the sediment cores 27, 28, 29, 30, 34 WP66 and 34 WP82 from San Antonio Bay. Top left map indicates the location of the cores. Note that cire 29 has multiple sand intercalations. Cores 30 and 34 WP82 have some clear shell fragments and (probably?) sand rich intervals indicating higher energy flow events.

Figure 5. Photos of the sediment cores 35, 36, 37 (San Antonio Bay) and 120 (Matagorda Bay – Colorado river mouth). Top left map indicates the location of the cores. Cores are dominated by muddy sediments with varied degrees of brown to grey alteration. Core 120 (PC-5 location on the map) was collected at the mouth of the Colorado River, and is characterized by homogenous silt and clay indistinctly layered at the base, which transitions to finely laminated organic-rich beds near the top. These observations of A) massive or indistinct bedding may relate to regular mixing at the mouth of the river, and B) punctual (i.e., seasonal) drought and flooding events.

Grain size analysis in cores

Understanding the accumulation and dynamics of microplastics in bay sediment is crucial, and key to this is analyzing the grain size and total organic content (TOC) of the sediment.

Grain size analysis on cores continued, completing analysis for cores 11, 13, 21, 31, 35, 36, and 37. Analysis was conducted at 2cm or 4cm intervals based on perceived variability from visual descriptions. The Mastersizer 3000, which uses laser diffraction to measure particle size distribution, was employed for this analysis (Malvern Panalytical, 2023).

We will now discuss the new cores analyzed in addition to the 65 sediment grab samples already examined in previous reports. The grainsize results from cores were presented as histograms (grain-size class frequency) with depth (Figures 6 to 12). Sediment grain size is primarily dominated by silts (between 4 and 60 microns), but there are some notable observations related to grainsize variability. While silt is the dominant grain size, some sampled cores (e.g., core 11, Fig. 6) exhibited dominance by very fine and fine sand. Another interesting finding is the presence of multiple high-frequency "peaks" in different grain size classes in many samples. For instance, samples at the surface (0 cm) and at depths of 4 cm and 8 cm in core 13 (Fig. 7) displayed three grain size peaks in clay silt and very fine sands. Many other samples in different cores have bi-modal or tri-modal distributions. This observation suggests that sediments transported by different processes are mixed in the deposits, possibly due to bioturbation or anthropogenic factors.

Some cores showed variability in grain size with depth. If no thin (mm) thick laminae were observed in the photos (Figs. 1 to 5), changes at the cm or dm scale are likely. For example, in core 21 (Fig. 8), while the core is predominantly silty, the bottom three samples (at depths of 24 cm, 26 cm, and 28 cm) are dominated by very fine sand. While most samples exhibit a tripartite distribution (clay-silt-very fine sand), some cores show variations with a higher peak of coarser sediments (very fine and fine sand).

The distribution of the predominant grain size (i.e., silt) is roughly similar to the findings of the last comprehensive survey (e.g., McGowen, 1979). Although the correlation between grain size, TOC content, and microplastics needs further analysis, no correlation was observed in previous sediment grab samples for which both microplastics and grainsize have been analyzed.

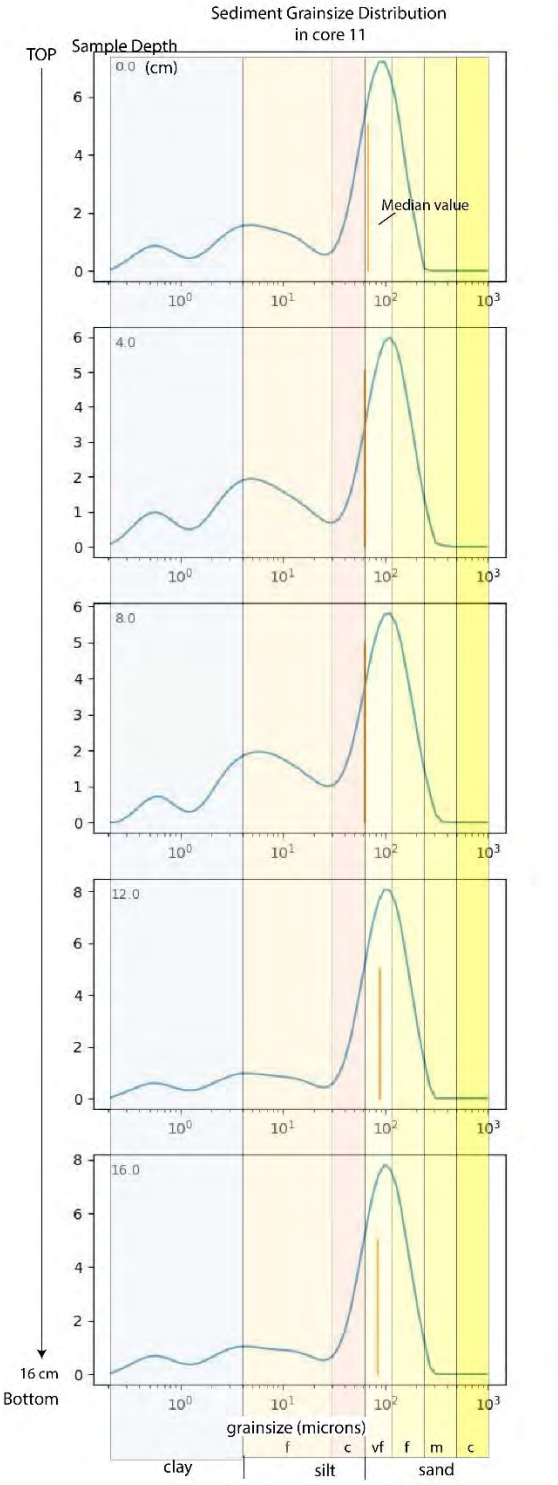

Figure 6. Sediment grain size in core 11. Multiple frequency histograms represent sediment samples at given depth in the core. On the X axis grainsize classes are separated and color coded to be easier to observe. The vertical orange line on each graph represents the median (d50) grain size value.

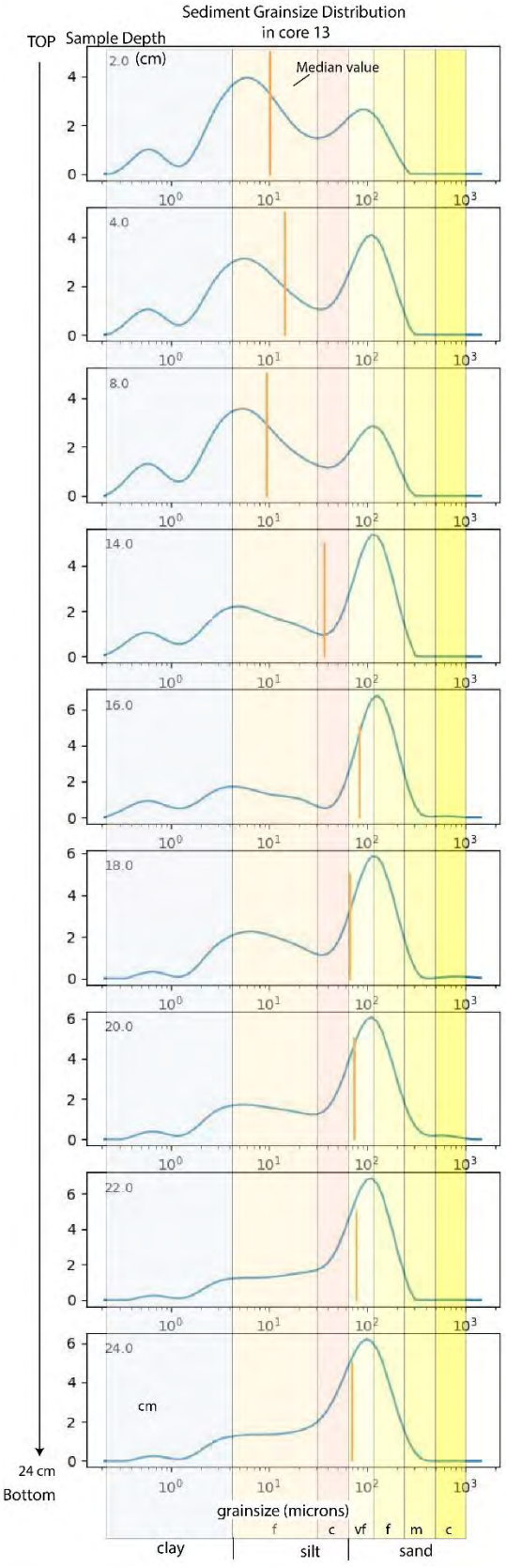

Figure 7. Sediment grain size in core 13. Multiple frequency histograms represent sediment samples at given depth in the core. On the X axis grainsize classes are separated and color-coded to be easier to observe.

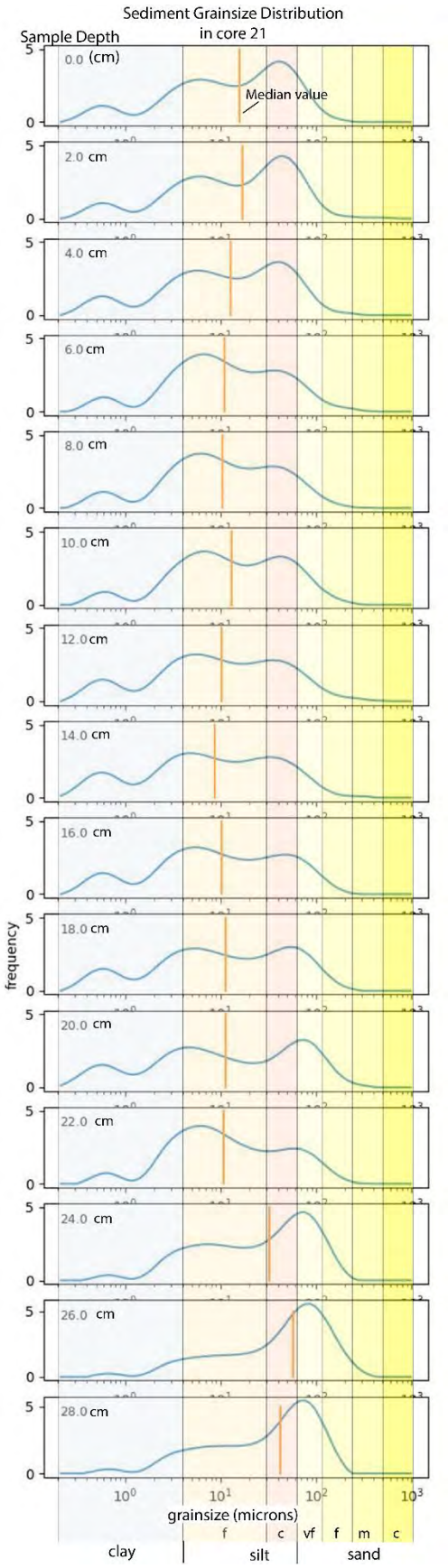

Figure 8. Sediment grain size in core 21. Multiple frequency histograms represent sediment samples at given depth in the core. On the X axis grainsize classes are separated and color-coded to be easier to observe.

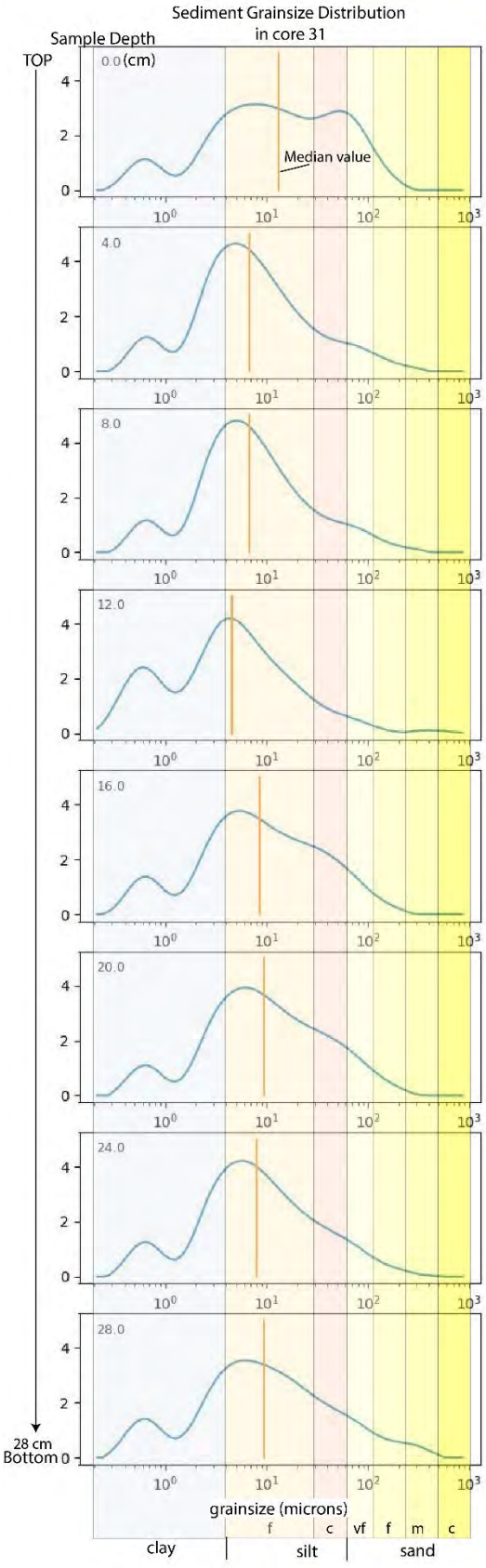

Figure 9. Sediment grain size in core 31. Multiple frequency histograms represent sediment samples at given depth in the core. On the X axis grainsize classes are separated and color-coded to be easier to observe

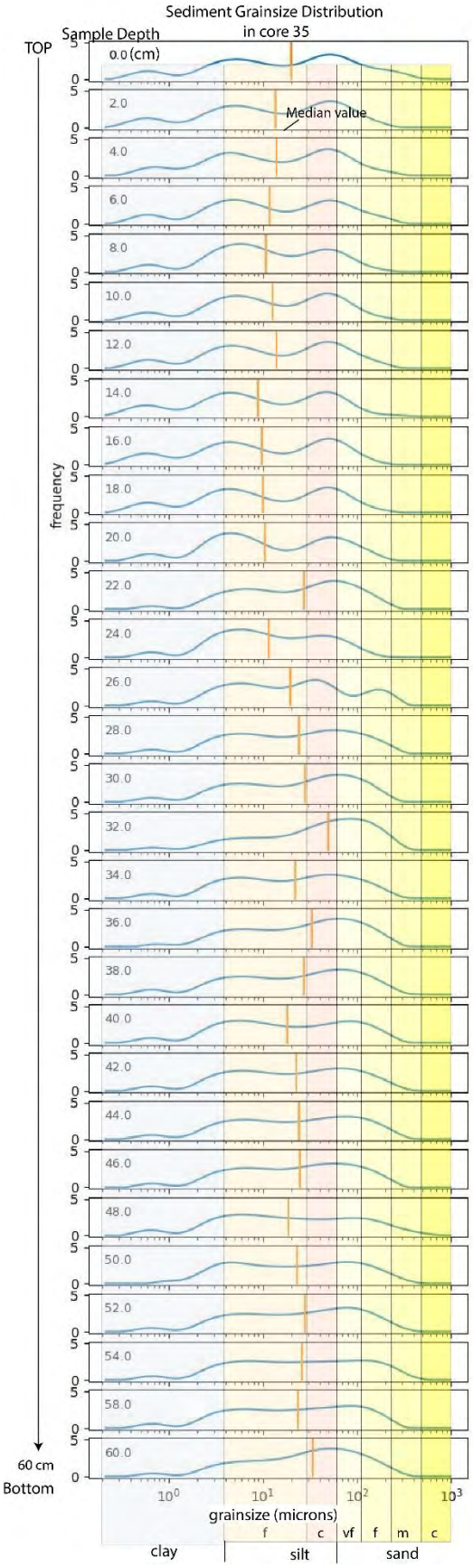

Figure 10. Sediment grain size in core 35. Multiple frequency histograms represent sediment samples at given depth in the core. On the X axis grainsize classes are separated and color-coded to be easier to observe

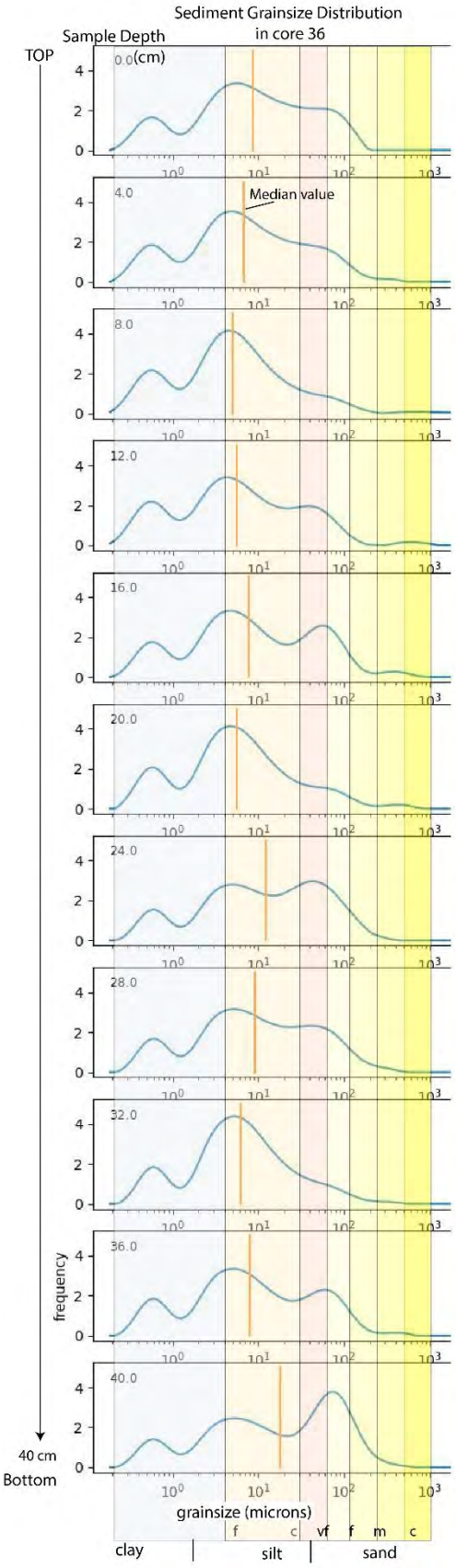

Figure 11. Sediment grainsize in core 36. Multiple frequency histograms represent sediment samples at given depth in the core. On the X axis grainsize classes are separated and color-coded to be easier to observe

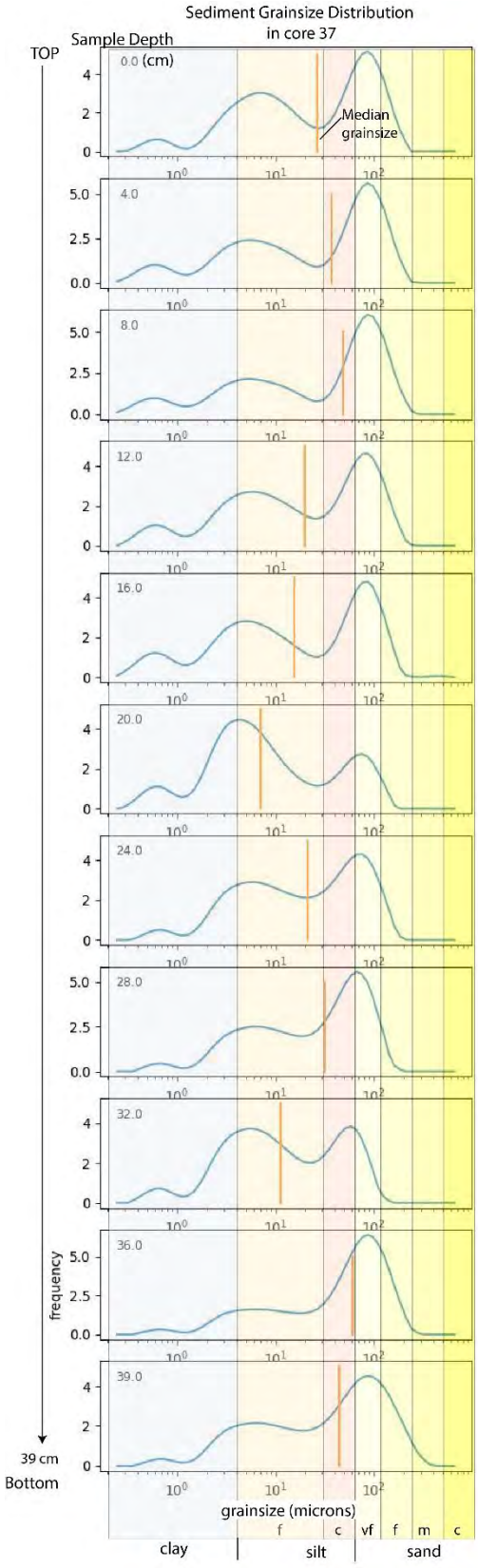

Figure 12. Sediment grainsize in core 37. Multiple frequency histograms represent sediment samples at given depth in the core. On the X axis grainsize classes are separated and color-coded to be easier to observe

The distribution of Total Organic Carbon (TOC) in Matagorda Bay was analyzed for all grab samples and for some of the cores. Understanding the association of organic carbon with microplastics is crucial, as organic material can serve as food for many organisms, and the presence or association of microplastics may harm fauna. To date, 65 grab samples from Matagorda Bay and the tops of cores have been analyzed for TOC content (see Table 1). Additionally, cores 11, 13, 21, 31, 35, 36, and 37 have also been analyzed for TOC. The overall variability in TOC values ranges from 0.2% to 3%, with most values falling between 0.8% and 2.2% TOC (refer to Fig. 13). These values are higher than the TOC values reported in McGowan's (1979) study, where most samples contained less than 0.5% TOC. This difference might be explained by increased of organic material accumulation in the bay caused by increased restricted circulation with the ocean. However, as previously mentioned, it also may be attributed to the different laboratory methods used, specifically Loss on Ignition in this study versus Wet Combustion in McGowan (1979) study.

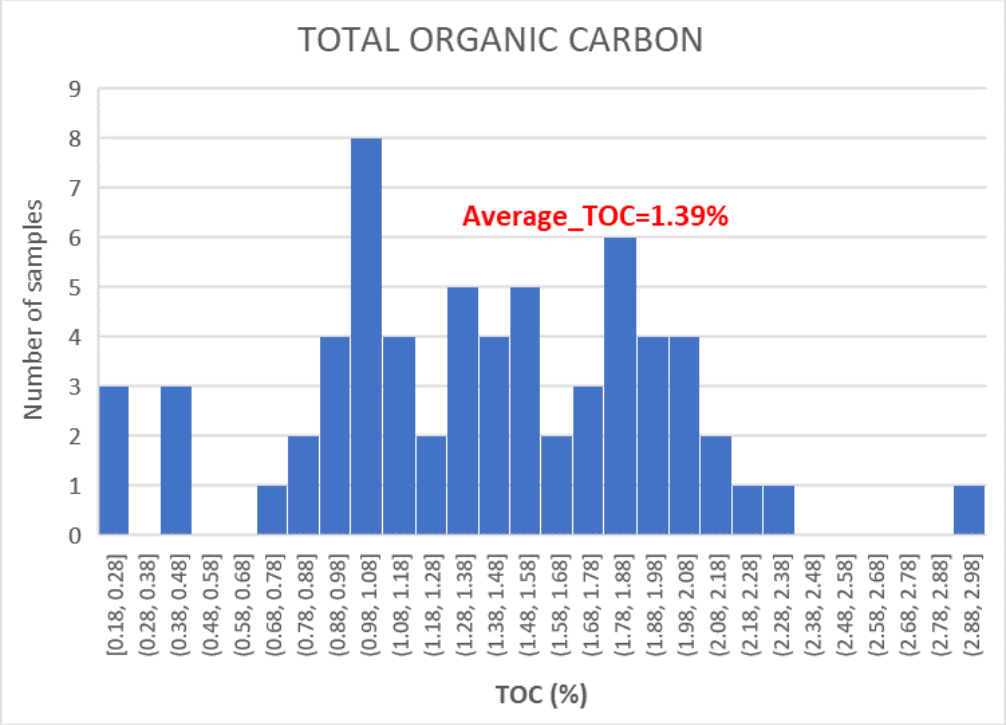

Figure 13 illustrates the distribution of Total Organic Carbon percentages in sediments at the bottom of the bay in grab samples and at the top of cores. The average TOC value is 1.39%.

SITE_NO	BAY_ID	GRAB_PCB	Weight Before (g)	Weight After (g)	LOI	TOC
25	SB	PCB	59.8309	59.0369	0.794	1.33
26	SB	PCB	59.4724	58.3169	1.1555	1.94
28	SB	PCB	57.1987	56.1167	1.082	1.89
29	SB	PCB	55.36	54.6306	0.7294	1.32
32	SB	G	52.7662	52.3874	0.3788	0.72
33	SB	G	52.9247	52.3687	0.556	1.05
35	SB	G	50.6248	49.4437	1.1811	2.33
36	SB	G	51.5946	50.6745	0.9201	1.78
37	SB	G	56.2862	55.4035	0.8827	1.57
38	SB	G	55.9598	55.3496	0.6102	1.09
39	SB	G	52.5624	51.9734	0.589	1.12
41	SB	G	56.659	56.1425	0.5165	0.91
42	SB	G	59.5536	58.8661	0.6875	1.15
43	SB	G	46.7374	46.1225	0.6149	1.32
44	SB	G	52.2988	51.6473	0.6515	1.25
45	SB	G	51.6719	51.0994	0.5725	1.11
46	SB	G	56.1625	55.1934	0.9691	1.73
47	SB	G	56.5523	55.8051	0.7472	1.32
48	SB	G	58.6492	58.0644	0.5848	1.00
49	SB	G	52.4013	51.5383	0.863	1.65
50	SB	G	54.8959	54.3625	0.5334	0.97
51	SB	G	59.6847	59.1105	0.5742	0.96
52	SB	G	53.9178	53.3664	0.5514	1.02
73	SB	G	55.9343	55.1293	0.805	1.44
79	SB	G	56.9131	56.8125	0.1006	0.18
6	MB	Water	46.6795	45.9756	0.7039	1.51
7	MB	G	51.9011	50.8297	1.0714	2.06
8	MB	G	50.6071	49.6669	0.9402	1.86
9	MB	G	49.1325	48.1601	0.9724	1.98
10	MB	G	47.9518	47.0551	0.8967	1.87
10	MB	G	59.1221	58.5391	0.583	0.99
12	MB	G	49.9354	49.2055	0.7299	1.46
13	MB	PCB	58.3742	57.7621	0.6121	1.05
13	MB	G	46.3092	45.7599	0.5493	1.19
14	MB	G	56.5449	55.7415	0.8034	1.42
15	MB	G	48.0055	47.0025	1.003	2.09
16	MB	PCB	53.0486	52.3661	0.6825	1.29
16	MB	G	49.4001	48.297	1.1031	2.23
17	MB	G	54.9539	54.071	0.8829	1.61
18	MB	G	47.6635	46.9388	0.7247	1.52
19	MB	PCB	59.336	59.0892	0.2468	0.42
19	MB	G	53.119	52.9863	0.1327	0.25
20	MB	G	56.425	55.2731	1.1519	2.04
21	MB	G	51.5643	50.6395	0.9248	1.79
22	MB	G	54.2982	53.8235	0.4747	0.87
23	MB	PCB	59.8593	59.3363	0.523	0.87
24	MB	G	50.0816	49.8865	0.1951	0.39
26	MB	PCB	48.7119	47.8236	0.8883	1.82
27	MB	G	52.3903	51.8768	0.5135	0.98
28	MB	G	53.472	53.2568	0.2152	0.40
29	MB	G	50.726	50.589	0.137	0.27
31	MB	G	58.1134	57.5524	0.561	0.97
32	MB	G	49.1332	48.2477	0.8855	1.80
33	MB	G	53.1903	52.6454	0.5449	1.02
34	MB	G	59.6734	58.7797	0.8937	1.50
120	MB	PCB	55.6482	54.5683	1.0799	1.94
1	EM	G	56.0222	55.4349	0.5873	1.05
2	EM	G	51.5035	50.5335	0.97	1.88
2	EM	G	51.4799	50.3838	1.0961	2.13
3	EM	G	51.4084	50.7088	0.6996	1.36
3	EM	PCB	50.6933	49.6578	1.0355	2.04
4	EM	PCB	54.9181	53.2876	1.6305	2.97
4	EM	G	46.714	46.0099	0.7041	1.51
5	EM	PCB	57.6937	56.6953	0.9984	1.73
44	EM	G	57.619	56.6009	1.0181	1.77

Table 1. Total Organic Carbon for the grab samples collected in Matagorda Bay (MB), East Matagorda Bay (EM), and San Antonio Bay (SB).

Sediment accumulation from bathymetry maps was also examined to better understand sediment dynamics in Matagorda Bay. Historical nautical charts from 1888, 1934, 1954, 1970, and 1981 (see Fig. 14) were digitized using ArcGIS software and re-gridded (see Fig. 15). Historical water depth values were subtracted between the different digital gridded maps and the modern NOAA depth soundings to quantify temporal changes and highlight the bay fill evolution.

The bathymetry differences map between 1888 and the present (see Fig. 16) indicates that Matagorda Bay has become shallower with more than 2 meters of sediment accumulation (red areas in Fig. 16), while some areas (green areas in Fig. 16) showed deepening behind the barrier. Most of the area towards the northeast accumulated sediments from the Colorado River, resulting in the bay becoming shallower. Interestingly, it appears that the bay has deepened behind the barrier bar, likely due to erosion of the bay shoreline, higher sediment compaction, subsidence in the area, or a combination of these factors (refer to Fig. 16).

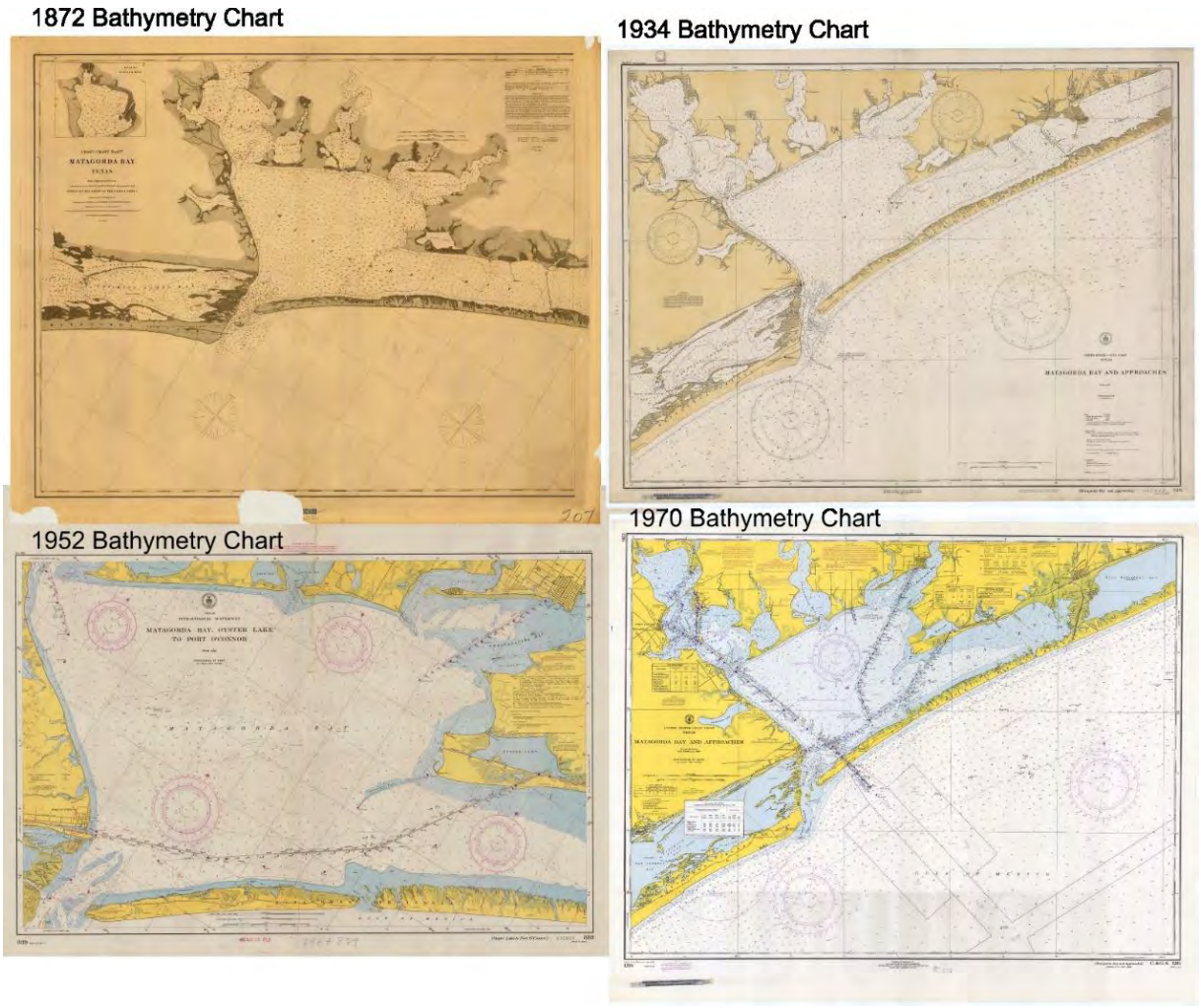

Figure 14 Historical navigation charts of Matagorda Bay from 1872, 1934, 1952 and 1970 that were digitized, re-gridded and used to observe the sediment accumulation/erosion patterns. Maps from 1888, 1981, and present are not shown.

Figure 15. Digized and re-gridded navigational bathymetric chart from 1888, depth units in meters.

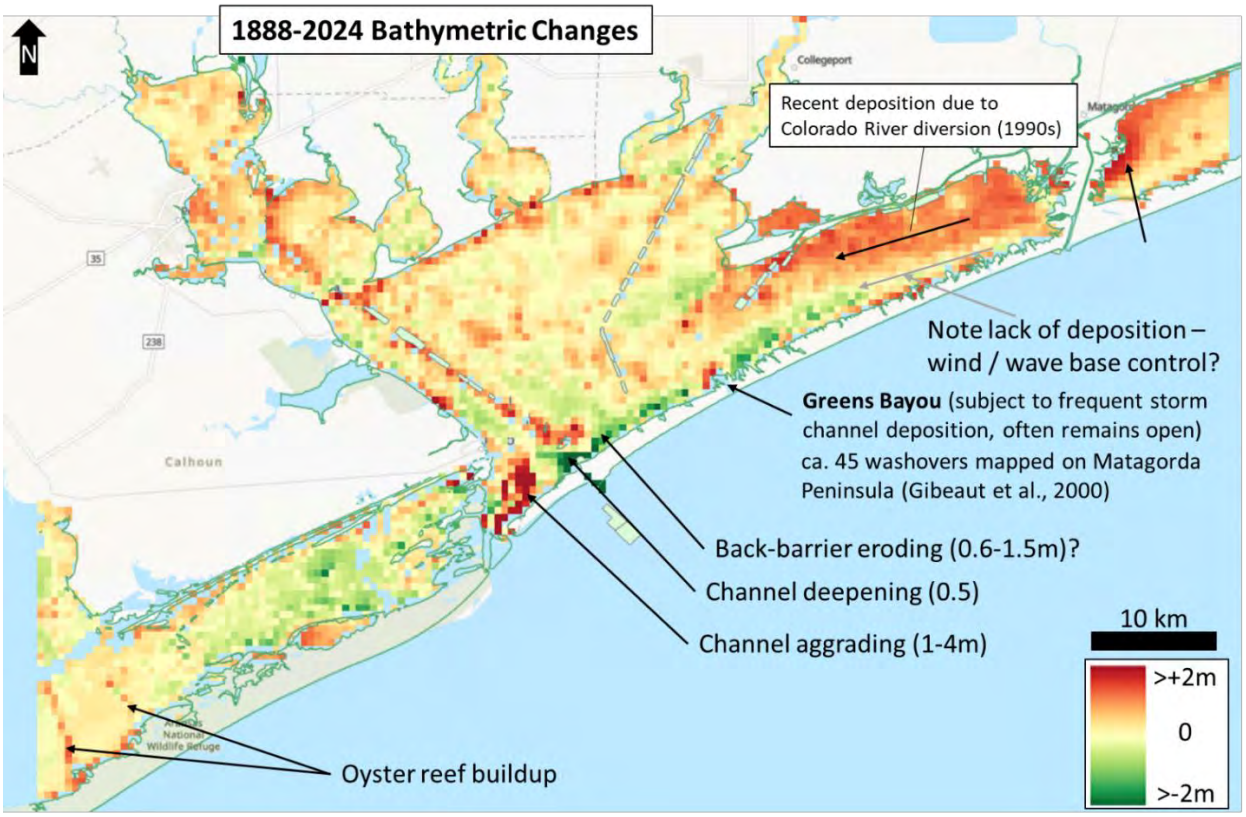

Figure 16. Map showing the water depth changes between 1888 and 2024 bathymetric maps. In areas with red bay got shallower, the sediments have been accumulated, in area with green the bay deepened, likely the sediments were eroded. Pale green rectangles indicate dredge spoil locations adjacent to ship channels (from NOAA, 2024).

Fieldwork conducted in September 2023 was centered on examining plastics in the surface water of Matagorda Bay. Utilizing a plankton net (see Figure 17), we collected surface water samples at eight offshore stations within the Matagorda and San Antonio bays. Currently, we are still processing these water samples, including digestion and subsequent analysis via Pyrolysis GC/MS. The forthcoming report will detail the occurrence, abundance, and distribution of microplastics within the surface water of Matagorda Bay during the 2023 study period.

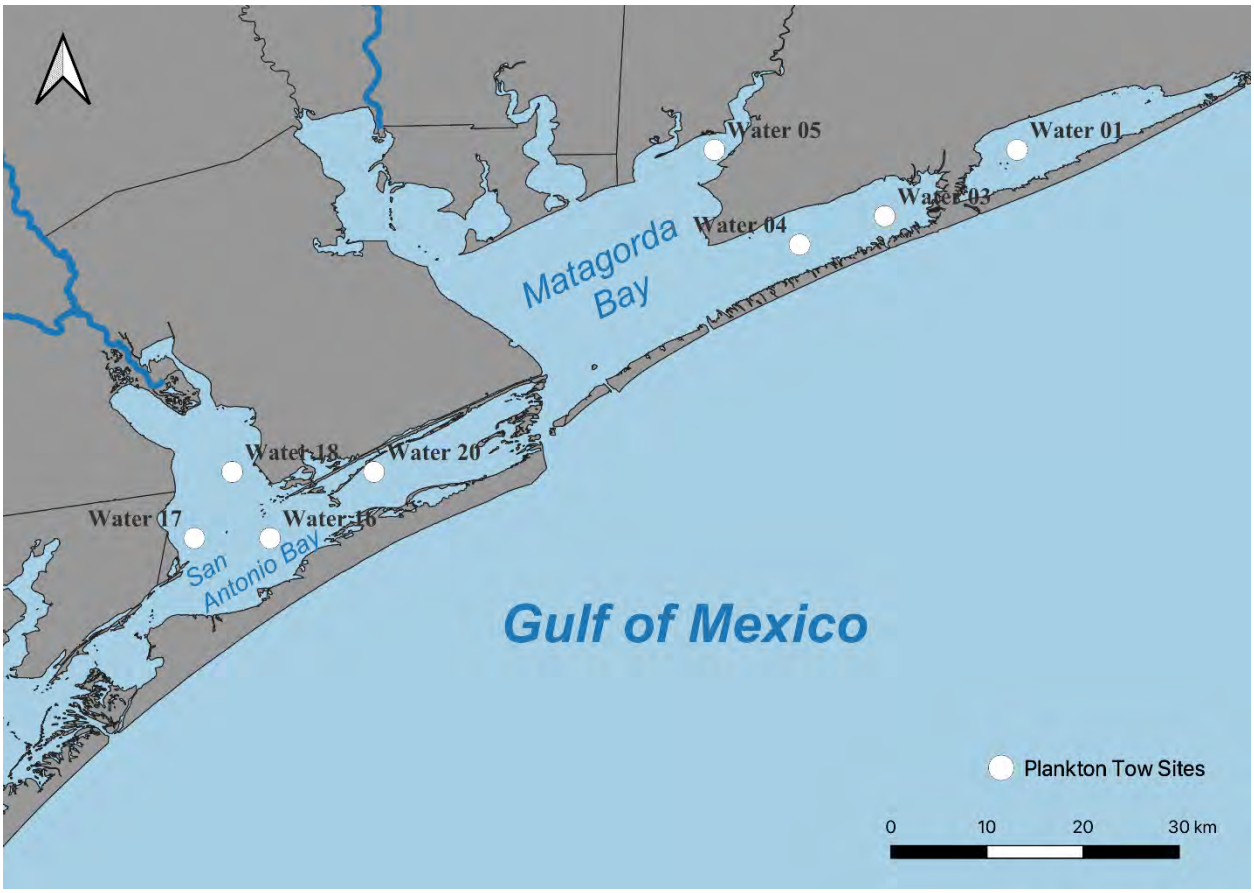

Figure 17. Sampling locations of surface water of Matagorda Bay and San Antonio Bay 2023.

Fieldwork conducted in December 2023 focused on the Colorado River Delta and adjacent area, located in the eastern part of Matagorda Bay. The Colorado River might be a source of microplastics because its catchment contains large urban areas. During this week-long campaign, sidescan and CHIRP data were collected to enhance our understanding of bathymetry and sedimentation in the Colorado Delta. Additionally, sediment grab samples were obtained to analyze the microplastic content of river-derived sediments accumulating in the bay (see Figs. 18 and 19).

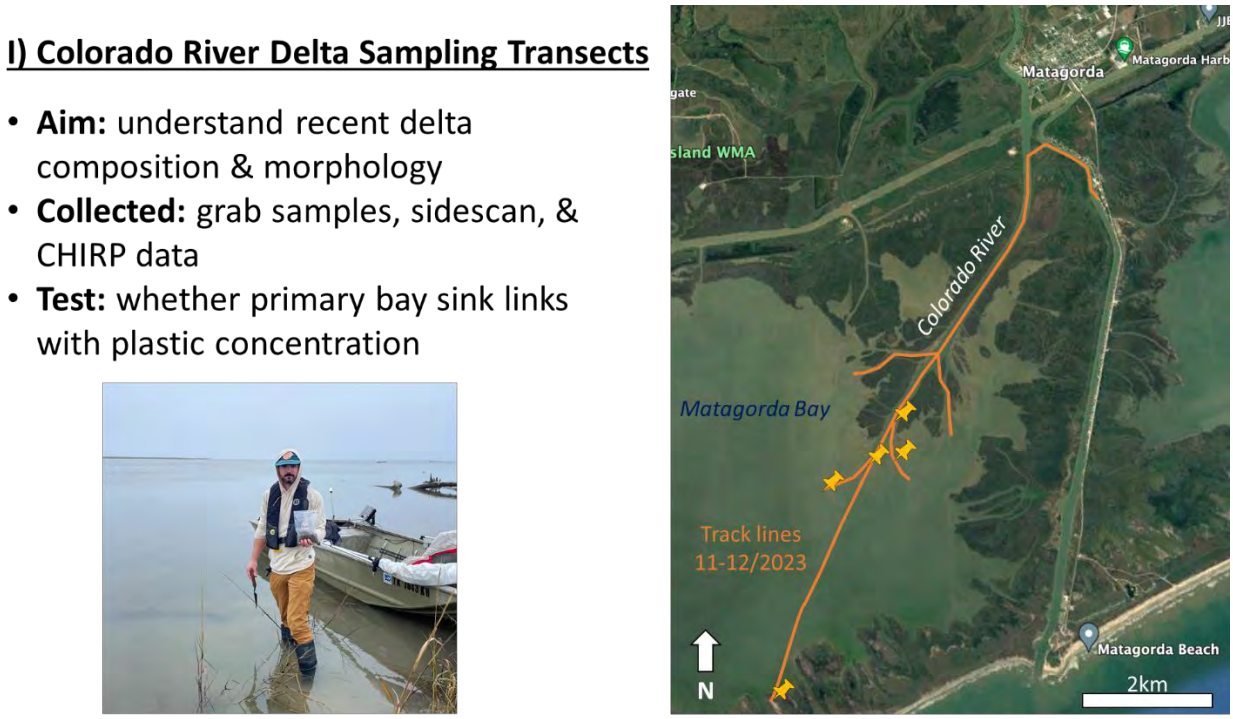

Figure 18. Data collected during December 2023 field work. Lower left photo show sediment data collected in delta front area of Colorado. On the right the lines of Chirp data and sediment sample locations.

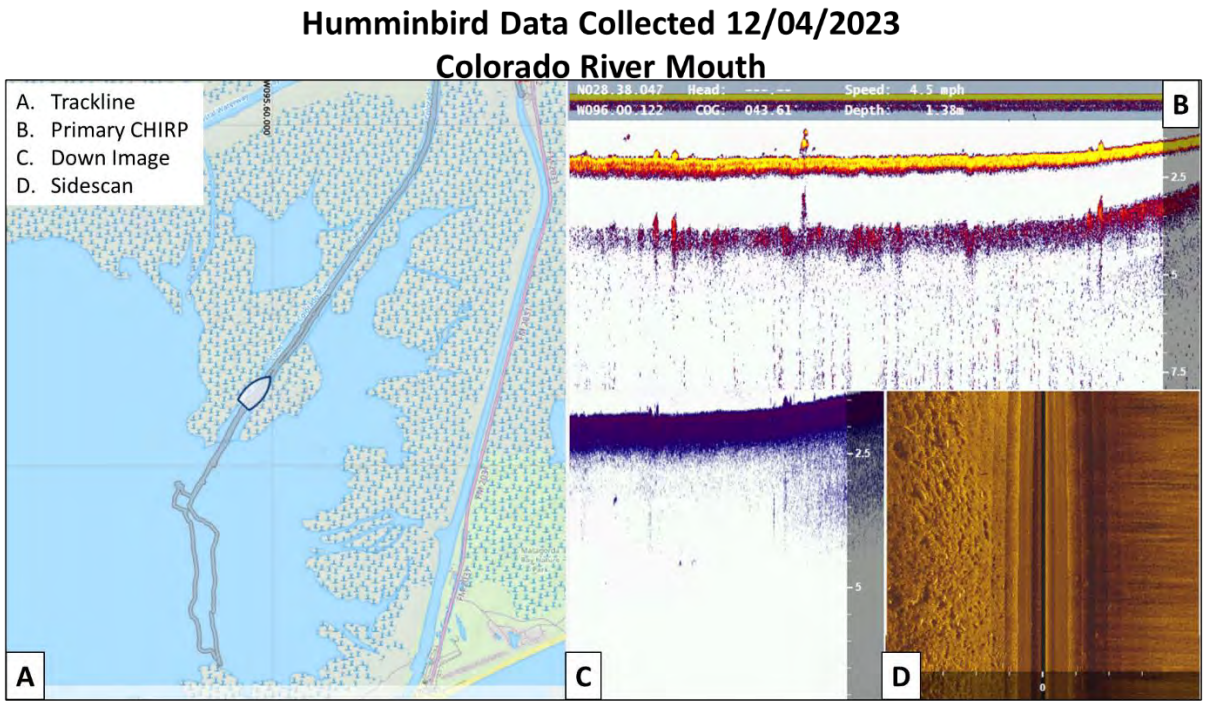

Figure 19. Example of CHIRP and Sidescan data collected along the Colorado Delta distributary channel.

The optimization of microplastic detection methods is currently underway. In response to the limited resolution of microscope FTIR for sediment and plankton tow samples, we are developing a state-of-the-art technique, the utilization of Pyrolysis GC/MS for the identification and quantification of microplastics. Various purification methods for isolating microplastics were evaluated, and plastic reference standards were procured from Frontier Laboratories Ltd (Japan). This commercial mixture contains 12 of the most prevalent types of plastics, including polyethylene, polypropylene, polystyrene, acrylonitrile butadiene styrene copolymer, styrene-butadiene copolymer, polymethyl methacrylate, polycarbonate, polyvinylchloride, polyethylene terephthalate, polyurethane, Nylon 6, and Nylon 66.

Subsequently, the separated microplastic samples will undergo analysis via pyrolysis GC/MS. The obtained results will be interpreted utilizing F-Search MPs (Frontier Lab Ltd.), an extensive database comprising pyrolyzates and polymer libraries (Fig. 20). This interpretation will facilitate both qualitative and quantitative analyses of microplastics by aligning the results with polymer standard calibration curves. Presently, we are in the process of establishing the standard calibration curves and determining the most effective purification method. This is also part of the key plan in the next project year should a no-cost extension be granted.

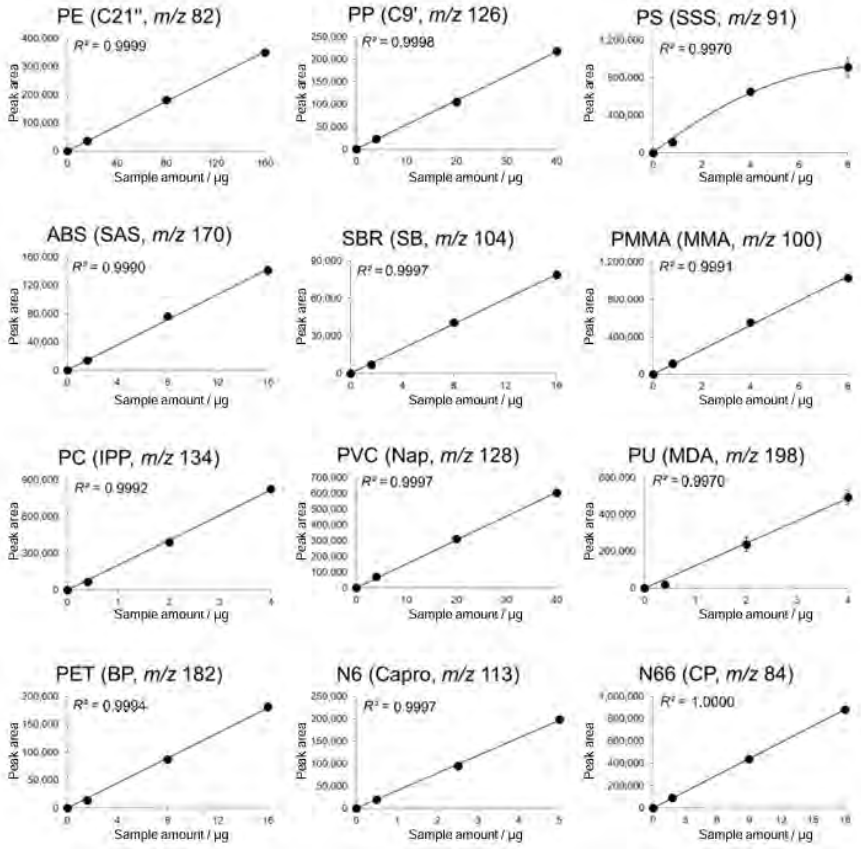

Table 1. Characteristic pyrolyzate for 12 polymers and LOD.

Polymer	Characteristic pyrolyzate*	*m/z*	LOD [µg]
PE	C21"	82	1.63
PP	C9'	126	0.54
PS	SSS	91	0.23
ABS	SAS	170	0.21
SBR	SB	104	0.38
PMMA	MMA	100	0.09
PC	IPP	134	0.06
PVC	Nap	128	0.51
PU	MDA	198	0.18
PET	BP	182	0.18
N6	Capro	113	0.10
N66	CP	84	0.35

* See previous note (PYA1-147E) for abbreviation.

Figure 20. Example of Calibration curves for 12 polymers created using microplastic standard kit. Adapted from Frontier technical note.

William Bailey presented the poster "*Characterization and Distribution of Microplastics in Texas Bays*" (shown below as a figure) at the American Geophysical Union Conference held in San Francisco, California in December 2023.

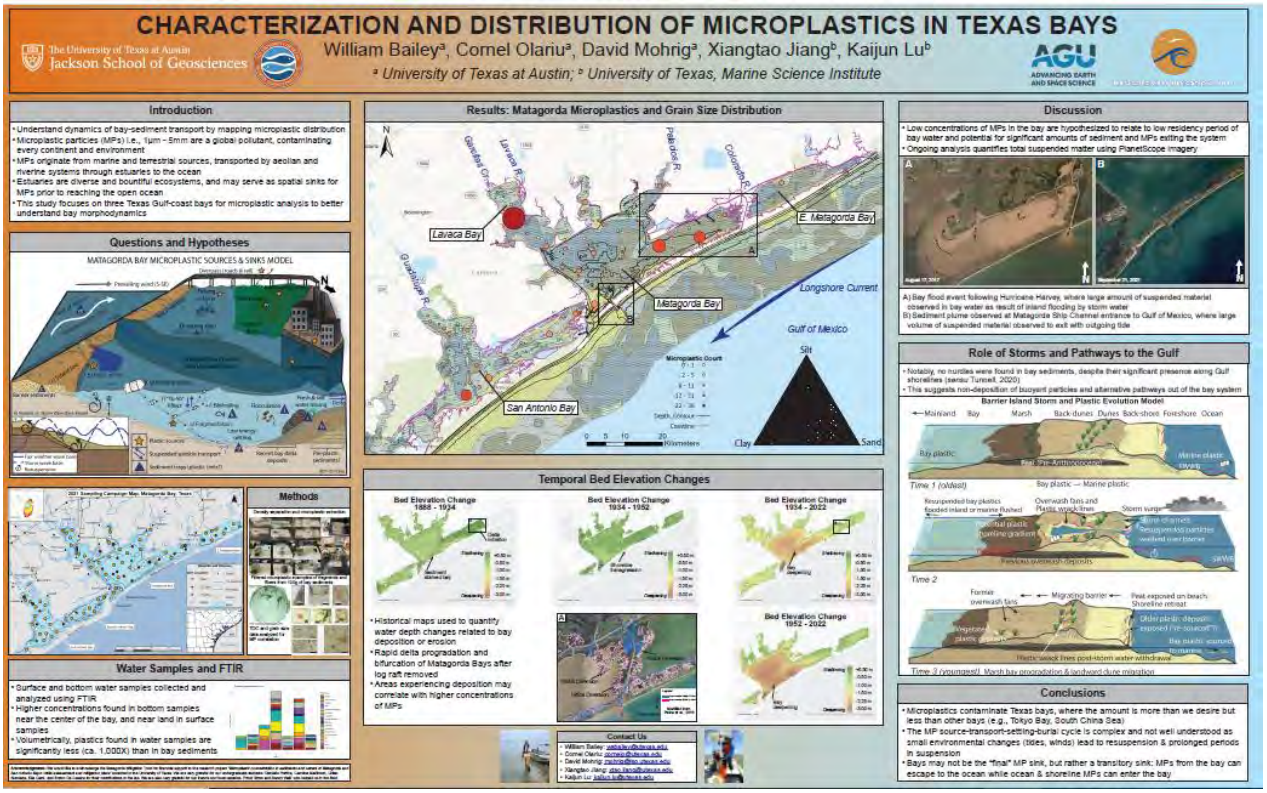

References

Gibeaut, J. C., White, W. A., Hepner, T., Gutierrez, R., Tremblay, T. A., Smyth, R., & Andrews, J. L. (2000). Texas Shoreline Change Project. Gulf of Mexico Shoreline Change from Brazos to Pass Cavallo.

McGowen, J. H. (1979). Geochemistry of bottom sediments--Matagorda Bay system, Texas. *Virtual Landscapes of Texas*.